www.czasopisma.pan.pl PAN POLSKA AKADEMIA NAUK www.journals.pan.pl

Arch. Metall. Mater.,Vol. 61 (2016), No 1, p. 347–352

DOI: 10.1515/amm-2016-0064

A. SZKLINIARZ*, W. SZKLINIARZ*, L. BLACHA*, G. SIWIEC*#

MICROSTRUCTURE OF HOT-DEFORMED Cu-3Ti ALLOY

In the paper, results of investigations regarding temperature and strain rate effects on hot-deformed Cu-3Ti alloy microstructure are presented. Evaluation of the alloy microstructure was performed with the use of a Gleeble HDS-V40 thermal-mechanical simulator on samples subjected to uniaxial hot compression within 700 to 900ºC and at the strain rate of 0.1, 1.0 or 10.0 s^{-1} until 70% (1.2) strain. It was found that within the analyzed temperature and strain rate ranges, the alloy deformation led to partial or complete recrystallization of its structure and to multiple refinement of the initial grains. The recrystallization level and the average diameter of recrystallized grains increase with growing temperature and strain rate. It was shown that entirely recrystallized, fine-grained alloy structure could be obtained following deformation at the strain rate of min 10.0 s^{-1} and the temperature of 800°C or higher.

Keywords: Copper-titanium alloy, hot deformation, microstructure, recrystallization

1. Introduction

Among copper alloys, precipitation-hardened Cu-Be alloys, called beryllium bronzes or beryllium copper, show the highest mechanical properties, very good corrosion and abrasion resistance, high electrical and thermal conductivity, non-sparking quality as well as good formability during hot and cold working. Beryllium bronzes are commonly used when sparking causes explosion hazard and for applications where good strength and conductivity as well as abrasion resistance, elasticity and corrosion resistance are required [1-12].

Essential disadvantages of beryllium bronzes are high prices and toxic properties. Due to their toxicity, the use of beryllium bronzes has been forbidden for many years in Poland and EU countries as beryllium compounds are hazardous during melting, casting, pressure welding, welding, hot deformation, cutting and grinding [1,13]. For many years, therefore, worldwide studies have been focused on discovering cheaper and non-toxic substitutes for Cu-Be alloys [1-12, 14]. Currently, the best substitutes for beryllium bronzes seem to be binary Cu-Ti or multicomponent Cu-Ti-X alloys that demonstrate mechanical properties and conductivity comparable to those of beryllium bronzes [15-17]. These alloys are suitable for precipitation hardening due to variable titanium solubility in solid copper [6, 7, 9, 11, 15, 16, 18-20]. It is estimated that over the next decade, these alloys, also called titanium bronzes or titanium copper, will effectively replace beryllium bronzes in most present applications.

The current global methods of manufacturing titanium bronze semi-finished and finished products are conventional techniques: melting and casting, hot and cold working as well as final treatment, i.e. solution heat treatment and aging, intended to ensure a required hardening level [3, 7, 11, 12, 21]. Sometimes, to obtain a higher hardening effect, the cold working process is performed between the solution heat treatment and aging processes [10, 22, 23].

The performance characteristics of titanium bronzes result from the titanium content, the size of matrix (copper-titanium solid solution) grain, overall deformation during cold working and morphologies of generated (during solution heat treatment and aging) dispersed precipitates of intermetallic phases [1-11, 14-23]. The matrix grain size, created during the hot working processes, markedly determines properties of titanium bronze semi-finished and finished products, affecting the course and effect of cold working as well as subsequent solution heat treatment and aging [2, 7, 23, 24].

Development of backgrounds for the technology of hot working of Cu-Ti ingots required investigations aimed at determining the best process conditions (temperature, strain rate and strain) to avoid cracking and to obtain fine, homogeneous matrix grain observed on the cross-section of semi-finished product being deformed.

The study objective was assessment of the potential for generating fine, homogenous grain on the cross-section of semi-finished products obtained from the Cu-3Ti alloy subjected to hot deformation at various temperatures and strain rates with the defined strain.

2. Experimental procedure

The investigated material was Cu-Ti alloy containing 3.0 % mass Ti. It was obtained with the use of a vacuum induction furnace [25-28] and cast to produce ingots (diameter: 40 mm, length: 350 mm). The ingots were subjected to 24-hour homogenising annealing at 850ºC, and then to hot

* SILESIAN UNIVERSITY OF TECHNOLOGY, FACULTY OF MATERIALS ENGINEERING AND METALLURGY, 8 KRASINSKIEGO STR., 40-019 KATOWICE, POLAND

Corresponding author: Grzegorz.Siwiec@polsl.pl

rolling at 950÷850ºC to yield rods of 12 mm in diameter. The rods were used for preparing samples for plastometric tests that were performed using a Gleeble HDS-V40 thermal-mechanical simulator during uniaxial hot compression at the strain rate of 0.1, 1.0 or 10.0 s^{-1} and the temperature of 700°C to 900°C. The rolling samples (diameter: 10 mm, height: 18 mm) were subjected to resistance heating at 3ºC/s under the vacuum to reach 950ºC. After 5-minute heating at that temperature, the samples were cooled at 10ºC/s to the defined deformation temperature and heated at that temperature for 1 minute, then compressed in a single run at the defined strain rate until the strain of 70% was obtained (corresponding to the true strain of 1.2). The stress changes versus strain were recorded. Following the deformation procedure, the samples were cooled in water. On the cross-sections of samples, their microstructure were determined by means of a Nikon Epiphot 200 microscope and HV hardness at 9.8 N by means of Zwick hardness tester.

The quantitative analysis of the microstructure was performed using the Met-Ilo software intended for image analyses [29, 30]. The following parameters were determined: the recrystallization level – the area fraction of recrystallized grains and the grain size – the average equivalent diameter of the grain plane section.

Preparation of material for microstructure investigations involved cutting with the use of an electrical discharge cutting-off machine, wet grinding, mechanical polishing on oxide and diamond pastes as well as etching in the mixture of 25 g ammonium persulphate and 100 ml H_2O and in the 15% HNO_3 solution.

The x-ray phase analysis was carried out by means of a Jeol JDX-7S diffractometer, using a lamp with a copper anode, powered by 20 mA, 40 kV current, and a graphite monochromator. The investigations were performed using a sample obtained from a hot-rolled rod, on the cross section perpendicular to the rod axis.

3. Results and discussion

Almost all flow curves of the Cu-3Ti alloy (Fig. 1), recorded during the plastometric tests, demonstrate a characteristic initial increase in flow stress (due to the hardening effect) to reach its maximum, followed by monotonic decrease (softening), suggesting the presence of structure rebuilding processes, mainly dynamic recrystallization, in the alloy being deformed. Higher temperatures result in lower strain. When it is reached, the structure rebuilding processes are initiated in the alloy. An exception is the flow curve recorded at 700°C (Fig. 1). In this case, when the maximum flow stress is reached, further alloy deformation occurs with practically unchanged stress, which proves that under these conditions, the effect of hardening due to deformation and softening due to the structure rebuilding, resulting from recovery and/or dynamic recrystallization, are in balance. Similar flow curves were recorded during compression at the strain rates of 0.1 and 1.0 s^{-1} [12].

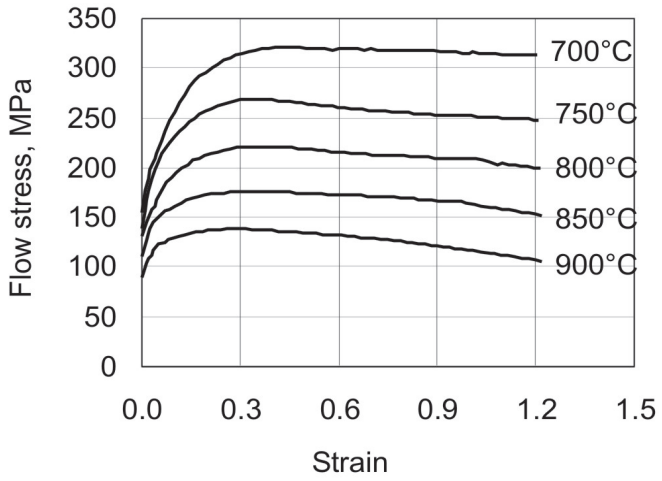

Fig.1. Flow curves at the strain rate of 10 s^{-1}

The Cu-3Ti alloy subjected to hot deformation demonstrates homogeneous, equiaxial grain microstructure (the average grain diameter: 72.3 µm) with numerous large precipitates at the grain boundaries and considerably smaller ones inside (Fig. 2). The x-ray analysis of the alloy phase composition showed its microstructure consisting of the grained phase α (copper-titanium solid solution) and, appearing as precipitates, the Cu_3Ti intermetallic phase (Fig. 3).

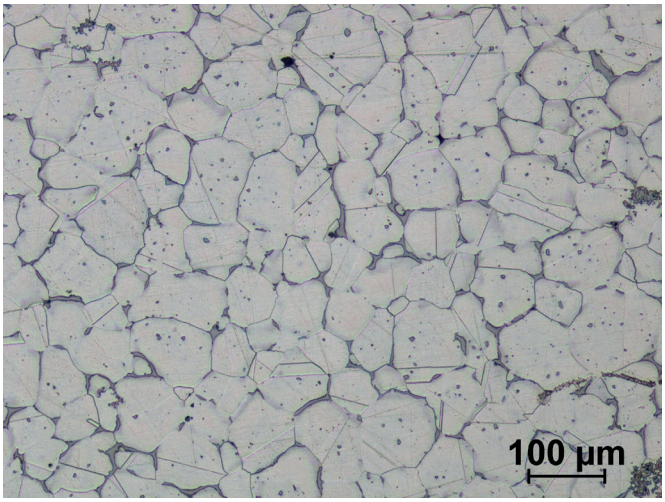

Fig. 2. Microstructure of Cu-3Ti alloy after hot rolling

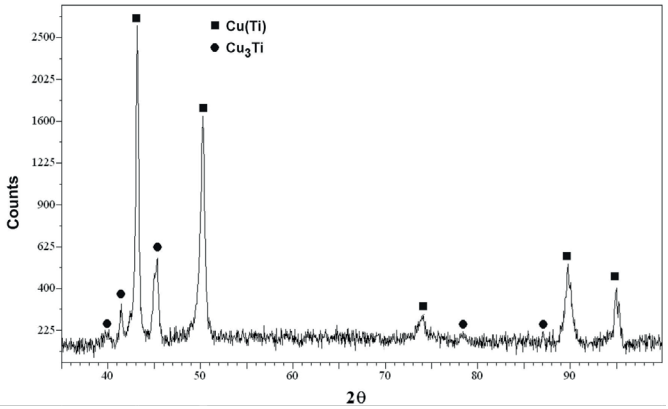

Fig. 3. The XRD diffraction spectra of Cu-3Ti alloy after hot rolling

This phase is not involved in further plastic deformation and structure rebuilding processes because during heat treatment, directly preceding the compression tests, that is performed at a temperature higher by nearly 200°C than the temperature of the upper limit of titanium solubility in copper (Fig. 4), it completely dissolves in the alloy matrix.

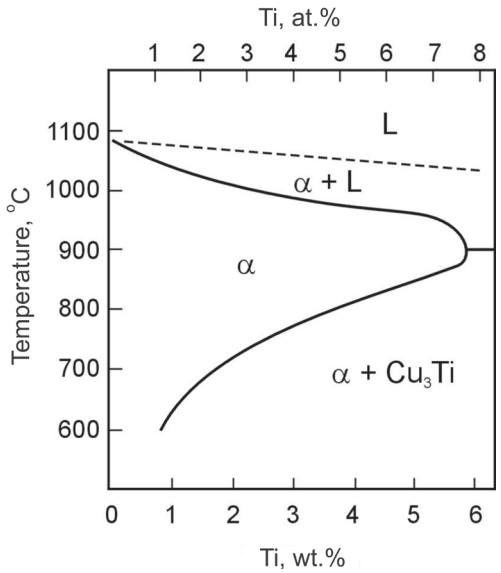

Fig. 4. Fragment of Cu-Ti phase diagram [4]

This is confirmed in Fig. 5a presenting the microstructure of alloy heated at 3°C/s up to 950°C, then heated at that temperature for 5 minutes and subsequently cooled in water. It did not show any precipitates of the Cu_3Ti intermetallic phase but far bigger grains of the average diameter of 94.5 µm (Figs. 2, 5a).

Cu-3Ti alloy deformation during compression at the strain rate of 0.1, 1.0 or 10.0 s^{-1} within 700 to 900°C occurs without cracking and leads to partial or complete recrystallization of its structure as well as to multiple refinement of the initial grains (Figs. 5, 6). The recrystallization level and the average diameter of new, recrystallized grains increase with growing temperature (Fig. 5). As shown for the alloy subjected to deformation at 700°C, the level of its structure recrystallization is also highly affected by the strain rate (Fig. 6). Deformation of the alloy at 700°C and a small rate of 0.1 s^{-1} results mainly in its hardening and microstructure consisting of deformed, elongated grains with recrystallization traces at their boundaries in the form of single new, fine grains (Fig. 6). Clear effects of dynamic recrystallization: new, fine grains forming characteristic chains around deformed old grains were observed following deformation at 700°C and 1.0 s^{-1}. For this temperature, however, only deformation at the rate of 10.0 s^{-1} resulted in a considerable structure recrystallization level above 80% (Fig. 6).

In Table 1, the effects of temperature and strain rate on the recrystallization level, average diameters of recrystallized

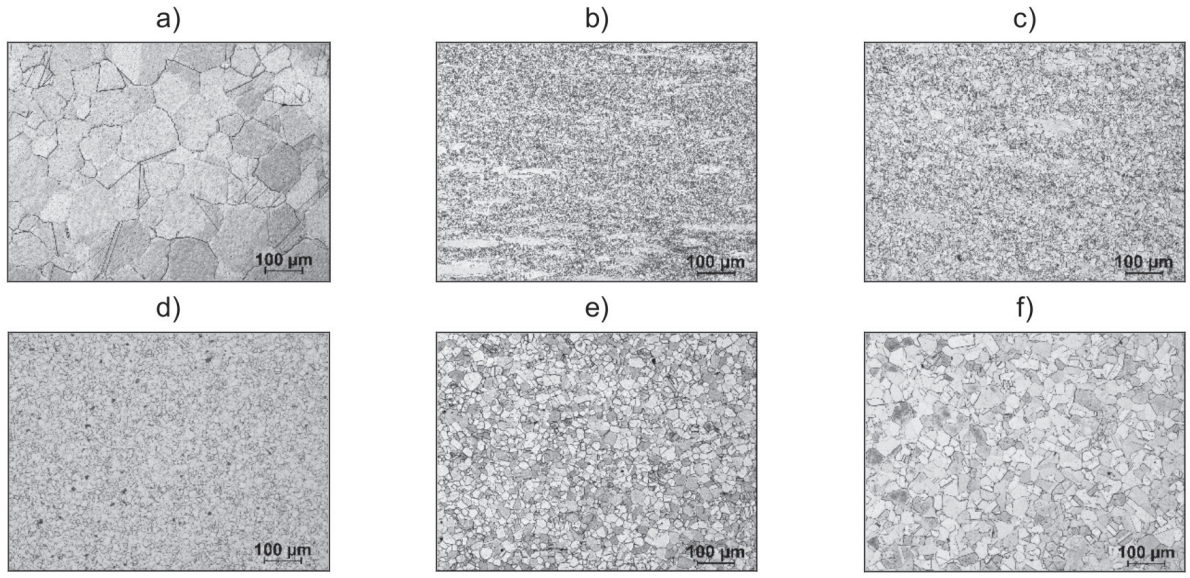

Fig. 5. Microstructure of alloy before deformation – 950°C/5 min./woda (a) and after deformation with strain rate of 10.0 s^{-1} at temperature: 700 (b), 750 (c), 800 (d), 850 (e) and 900°C (f)

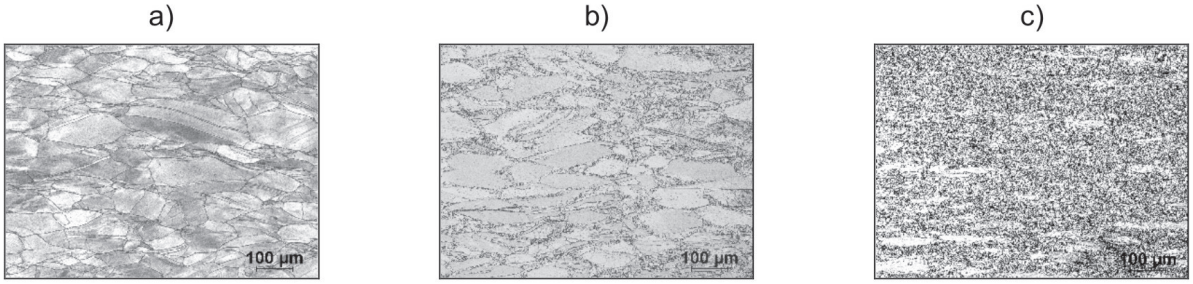

Fig. 6. Microstructure in the middle area of sample after deformation at temperature of 700°C and at strain rate of: 0.1 (a), 1.0 (b), 10.0 s^{-1} (c)

grains and hardness of the investigated alloy are presented. The data show that the rise in temperature and strain rate leads to a significantly increased structure recrystallization level. A completely recrystallized structure is obtained after deformation at the temperature of 800°C or higher, providing that the strain rate is 10.0 $s^{-1.}$ Deformation at smaller rates, regardless of the applied temperature within 700÷900°C, never results in complete structure recrystallization (Table 1). The average diameter of recrystallized grains markedly increases with growing deformation temperature, particularly in the case of complete recrystallization. For a given temperature, a higher strain rate leads to a significant increase in the recrystallization level and a small rise in the average diameter of recrystallized grains, which is reflected by lower hardness of the alloy being deformed (Table 1).

The macrostructure presented in Fig. 7 shows that in the process of compression (upsetting), a three-dimensional stress state is observed that causes non-uniform deformation within the sample volume. The longitudinal section of a cylindrical sample subjected to upsetting demonstrates three deformation areas (Fig. 7):

- Area A — directly on the side of the deformed sample surface contact with the applied tool — the area of minor deformation due to friction that prevents side flow
- Area B — inside the sample — the area where major axial and radial types of deformation are observed
- Area C — directly on the side of the sample lateral surface — the area of medium deformation due to peripheral tensile stress.

TABLE 1

Effect of deformation parameters on the microstructure and hardness of Cu-3Ti alloy

Temperature °C	Strain rate, s^{-1}	Recrystallizations degree, %	Average grain diameter, µm	Hardness VHN/1
700	0.1	2.0	6.8	375
	1.0	8.2	7.6	307
	10.0	39.8	9.8	254
750	0.1	25.7	10.9	263
	1.0	31.2	10.8	261
	10.0	75.4	12.8	236
800	0.1	36.3	13.4	254
	1.0	50.5	14.9	247
	10.0	100.0	15.2	232
850	0.1	45.4	18.5	250
	1.0	63.6	19.4	242
	10.0	100.0	20.9	225
900	0.1	78.2	25.4	233
	1.0	90.8	28.3	228
	10.0	100.0	28.2	224

TABLE 2

Effect of deformation parameters on the microstructure homogeneity and hardness of Cu-3Ti alloy

Deformation parameters	Deformation zone	Degree of recrystallization, %	Average grain diameter, µm	Hardness VHN/1
700°C 0.1 s^{-1}	A	0.6	7.2	393
	B	4.0	6.4	356
	C	1.4	6.8	376
700°C 10.0 s^{-1}	A	11.4	10.2	273
	B	83.6	9.4	232
	C	24.5	9.8	257
750°C 10.0 s^{-1}	A	54.8	13.1	244
	B	86.9	12.5	231
	C	84.5	12.8	233
800°C 10.0 s^{-1}	A	100.0	16.0	228
	B	100.0	14.3	236
	C	100.0	15.3	232
850°C 10.0 s^{-1}	A	100.0	23.4	220
	B	100.0	17.3	230
	C	100.0	22.0	225
900°C 10.0 s^{-1}	A	100.0	34.5	219
	B	100.0	23.5	225
	C	100.0	26.6	228

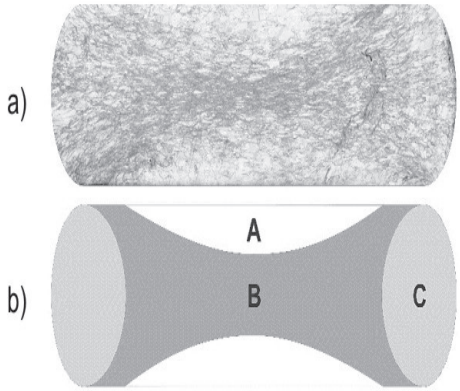

Fig. 7. Macrostructure of Cu-3Ti alloy after deformation at temperature of 750°C with strain rate of 0.1 s^{-1} (a) and scheme of area occurrence of: minor (A), large (B) and medium (C) deformation (b)

Transition between the particular areas is continuous without a clearly marked boundary. The existing areas result in inhomogeneous microstructure with various recrystallization levels and different grain sizes. The microstructure inhomogeneity is a result of the applied temperature and strain rate (Fig. 8, Tab. 2). In the case of samples subjected to deformation at 0.1 and 1.0 s^{-1} within 700÷900°C as well as at 10.0 s^{-1} within 700÷750°C, the microstructure inhomogeneity refers to the recrystallization level and average grain diameters, while for the samples subjected to deformation at 10.0 s^{-1} within 800÷900°C, i.e. with complete recrystallization, the microstructure is only inhomogeneous in terms of the average grain diameters.

In the cases of incomplete recrystallization (deformation at 0.1 and 1.0 s^{-1} within 700÷900°C as well as at 10.0 s^{-1} within 700÷750°C), the most recrystallized structure is observed in the area of major deformation (area B) and the least recrystallized structure is found in the area of minor deformation (area A). Growing temperature and strain rate result in higher levels of recrystallization in the particular areas of the sample being deformed (Fig. 8, Tab. 2).

Regardless of the applied temperature and strain rate, the smallest grains are found in the area of major deformation (area B), the medium-sized grains – in the area of medium deformation (area C) and the largest ones – in the area of minor deformation (area A). Temperature rise leads to successive increase in the average grain diameters in respective areas of

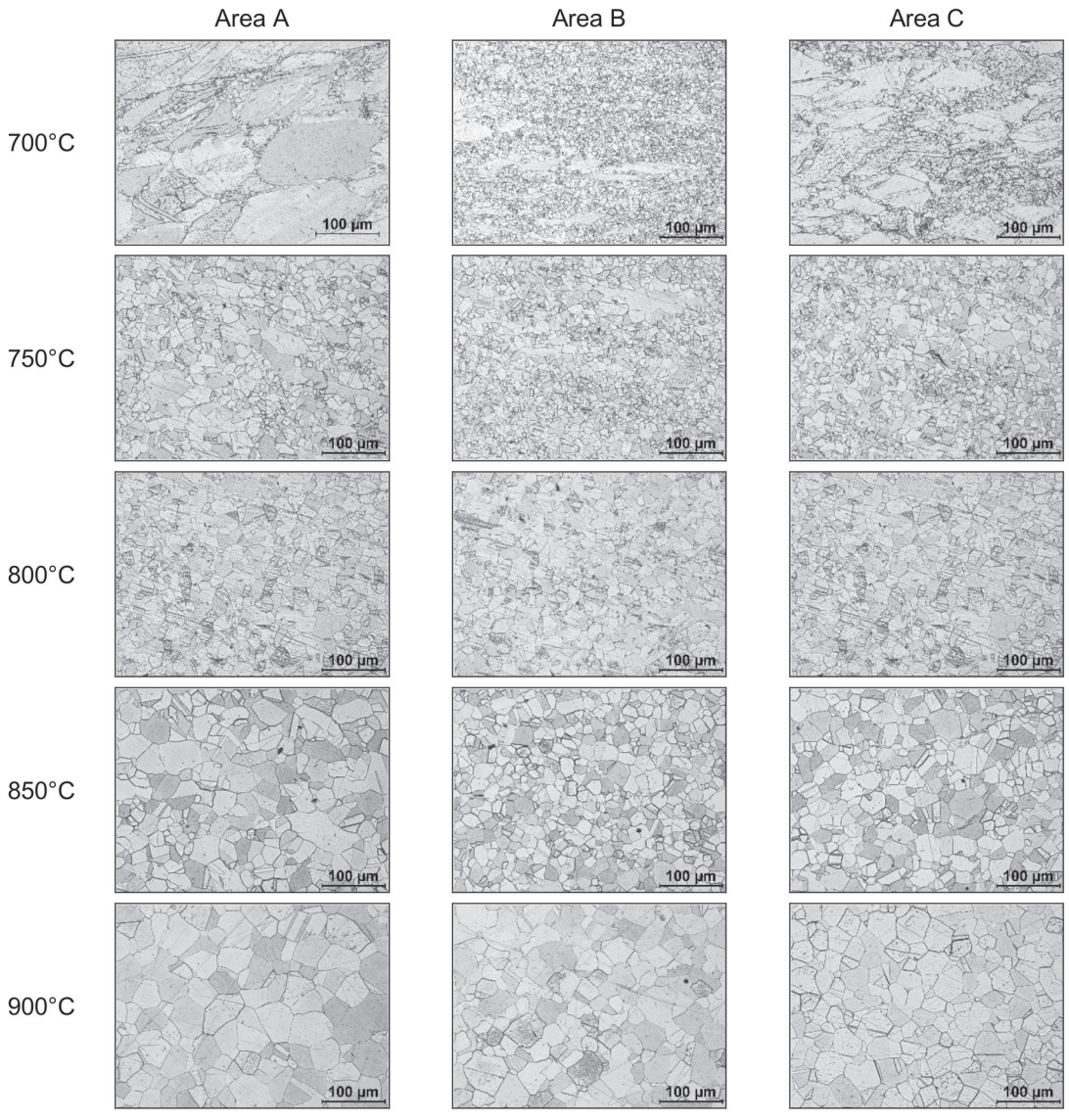

Fig. 8. Microstructure of particular areas of sample (Fig. 7b) after deformation at strain rate of 10.0 s^{-1} at different temperature

the sample (Tab. 2, Fig. 8). The rate of average grain diameter increase in the particular sample areas with growing temperature of deformation is different. This leads to increasingly high non-uniformity of grains seen in the microstructure on the cross-section of the sample subjected to deformation at rising temperature. Inhomogeneity of grain sizes, enhanced when the deformation temperature rises, proves that the stage of primary recrystallization has been completed and the stage of grain growth has begun. Inhomogeneity of grain sizes in the particular areas, observed following hot deformation, is a disadvantage reflected in the process of subsequent cold working that results in diverse microstructure and properties on the cross-section of produced semi-finished product.

For samples that are deformed under conditions of incomplete recrystallization, enhancement of recrystallization levels in the particular areas leads to reduced alloy hardness. The same effect is seen for increased average diameters of grains in the particular areas of the sample subjected to deformation with complete recrystallization (Tab. 2).

4. Conclusions

The flow curves, representing stress changes versus true strain for the Cu-3Ti alloy subjected to hot compression at 700–900°C, are a sum of counter effects of the hardening process due to deformation and softening caused by processes of structure rebuilding, mainly dynamic recrystallization.

Cu-3Ti alloy deformation during compression at the strain rate of 0.1, 1.0 or 10.0 s^{-1} within 700 to 900°C leads to partial or complete recrystallization of its structure as well as to over 6-fold refinement of the initial grains. A completely recrystallized structure is obtained after deformation at the strain rate of 10.0 s^{-1} and the temperature of 800°C or higher.

The recrystallization level and the average diameter of recrystallized grains increase with growing temperature and strain rate. Enhancement of the recrystallization level and grain refinement result in, respectively, increased or reduced hardness of the alloy subjected to hot deformation.

The deformation process on the cross-section of compressed sample is non-uniform, resulting in inhomogeneity of the strain in its particular areas and, therefore, diverse recrystallization levels and grain sizes.

The investigations has shown that the Cu-3Ti alloy should be subjected to deformation at the temperature of 800°C and the strain rate of at least 10.0 s^{-1}, which ensures that the completely recrystallized structure and the smallest grains are obtained. Lower temperatures of deformation are not recommended due to incomplete recrystallization of the structure, while higher temperatures — due to undesired grain growth and enhancement of grain non-uniformity on the cross-section of the semi-finished product being subjected to deformation.

Acknowledgment

This work was partially financed by a grant The National Centre for Research and Development of Poland No R1500402

Received: 10 March 2015.

REFERENCES

[1] Z. Rdzawski, Alloyed copper (in Polish), Silesian University of Technology House of Publishing, Gliwice (2009).
[2] S. Nagarjuna, M. Srinivas, K. Balasubramanian, D.S. Sarma, Acta Metall. Mater. **44**, 2285-2293 (1996).
[3] S. Nagarjuna, K. Balasubramanian, D.S. Sarma, Mat. Sci. Eng. A **225**, 118-124 (1997).
[4] S. Nagarjuna, M. Srinivas, K. Balasubramanian, D.S. Sarma, Int. J. Fatigue **19**, 51-57 (1997).
[5] S. Nagarjuna, M. Srinivas, K. Balasubramanian, D.S. Sarma, Mat. Sci. Eng. A **259**, 34-42 (1999).
[6] S. Suzuki, K. Hirabayashi, H. Shibata, K. Mimura, M. Isshiki, Y. Waseda, Scripta Mater. **48**, 431-435 (2003).
[7] W.A. Sofa, D.E. Laughlin, Prog. Mater. Sci. **49**, 347-366 (2004).
[8] S. Nagarjuna, M. Srinivas, Mat. Sci. Eng. A **406**, 186-194 (2005).
[9] S. Semboshi, T. Nishida, H. Numakura, Mat. Sci. Eng. A **517**,105-113 (2009).
[10] S. Semboshi, S. Orimo, H. Suda, W.L. Gao, A. Sigawara, Mater. Trans. **52**, 2137-2142 (2011).
[11] S. Semboshi, T. Takasugi, J. Alloy Compd. **580**, 397-400 (2013).
[12] A. Szkliniarz, L. Blacha, W. Szkliniarz, J. Łabaj, Archives of Metallurgy and Materials **59** (4), 1113-1118 (2014).
[13] M. Madej, Bezpieczeństwo pracy nauka i praktyka **5**, 26-28 (1999).
[14] S. Nagarjuna, M. Srinivas, Mat. Sci. Eng. A **335**, 89-93 (2002).
[15] S. Nagarjuna, K.K. Sharma, I. Sudhakar, D.S. Sarma, Mat. Sci. Eng. A 313, 251-260 (2001).
[16] S. Nagarjuna, D.S. Sarma, J. Mater. Sci. **37**, 1929-1940 (2002).
[17] F. Wang, Y. Li, K. Wakoh, Y. Koizumi, A. Chiba, Mater. Des. **61**, 70-74 (2014).
[18] D.E. Laughlin, J.W. Cahn, Acta Metall. Mater. **23**, 329-339 (1975).
[19] H. Okamoto, J. Phase Equilib. **23** (3), 549-550 (2002).
[20] L. Blacha, G. Siwiec, A. Kościelna, A. Dudzik-Truś, Inżynieria Materiałowa 6 (172), 520-524 (2009).
[21] A.A. Hameda, L. Blaż, Mat. Sci. Eng. A **254**, 83-89 (1998).
[22] S. Nagarjuna, K. Balasubramanian, D.S. Sarma, J. Mater. Sci. **34**, 2929-2942 (1999).
[23] S. Nagarjuna, M. Srinivas, Mater. Sci. Eng. A **498**, 468-474 (2008).
[24] S. Nagarjuna, M. Srinivas, K. Balasubramanian, D.S. Sarma, Scripta Metall. **30**, 1593-1597 (1994).
[25] A. Szkliniarz, W. Szkliniarz, Solid State Phenom. **176**, 139-148 (2011).
[26] A. Szkliniarz, Solid State Phenom. **176**, 149-156 (2011).
[27] L. Blacha, J. Łabaj, Metalurgija **51** (4), 529-533 (2012).
[28] G. Siwiec, Archives of Metallurgy and Materials **58** (4), 1155-1160 (2013).
[29] J. Szala, Application of Computer-Aided Image Analysis for Quantitative Evaluation of Materials' Structure (in Polish), Silesian University of Technology House of Publishing, Gliwice (2001).
[30] W. Szkliniarz, A. Szkliniarz, Solid State Phenom. **197**, 113-118 (2013).